Cement and Concrete Research 39 (2009) 696–700

Contents lists available at ScienceDirect

Cement and Concrete Research

journal homepage: http://ees.elsevier.com/CEMCON/default.asp

Hilbert transformation of waveforms to determine shear wave velocity in concrete

Recep Birgül *

Department of Civil Engineering, College of Engineering, Mugla University, Mugla, 48100, Turkey

ARTICLE INFO

Article history:
Received 16 January 2008
Accepted 14 May 2009

Keywords:
Nondestructive (new)
Elastic moduli (C)
Physical properties (C)
Concrete (E)

ABSTRACT

Given the density value, elastic properties of a homogeneous and isotropic material can be determined provided that primary and shear wave (P- and S-wave) velocities are known. P-waves are easier to monitor and detect compared to the S-waves. In concrete, along with P-wave velocity, shear wave velocity measurement is important in determining the elastic properties. These elastic properties could be implemented in assessing the quality of in-situ concrete. After an extensive literature survey, this study focused on the applicability of Hilbert transformation of waveforms to determine shear wave velocity in concrete material. The experimental work consisted of a set of ultrasonic measurements on the surface of a reinforced concrete deck. The recorded waveforms were then analyzed to obtain the arrival times of P- and S-waves. Hilbert transformation of the waveforms proved to yield reliable and repeatable results.

1. Introduction

Concrete is known to be the most widely used material in the construction industry. For the quality control and quality assurance of concrete, destructive tests are often performed to assess the properties of in-situ concrete. However, it has become increasingly evident that utilizing non-destructive test methods are more practical and cost effective in material evaluation [1–9]. Non-destructive testing makes it possible to obtain changes in concrete properties with time and external effects; thus it is plausible to use non-destructive testing in quality control and quality assurance [10–16].

Among the many non-destructive test methods, the ones based on stress wave propagation are utilized to assess the mechanical properties of a material. One of those non-destructive tests is ultrasonic pulse velocity (UPV) determination which relates to material properties such as porosity, permeability and elasticity modulus [6,11,17–20]. However, because of its heterogeneous nature, assessing the in-situ properties of concrete is quite difficult through ultrasonic testing.

Theoretically, for a homogeneous and isotropic material the two independent elastic constants, elasticity modulus and Poisson's ratio, can be determined with the measured primary wave and shear wave velocities (P- and S-waves) together with the density of the material [1,2]. As the P-wave is the fastest wave, it is widely used in material property characterization. On the other hand, S-waves are slower and difficult to determine as reflected, refracted or scattered waves most often hinder the arrival of these waves [14]. Therefore, research on the use of shear waves in concrete material is rare, possibly because utilizing shear waves is difficult even in steel materials [21–23].

Several analysis techniques, both in time and frequency domains, were considered to determine the S-wave velocity of concrete material [24–31]. These techniques had been primarily developed for geotechnical applications. Since both concrete and soil are known as heterogeneous materials, these techniques might have been applicable to concrete material as well. Among the methods considered, impulse-response, resonant column, and spectral analysis of surface wave methods required special equipment and geometry of material in question, therefore discarded [32,33]. Other techniques of determining the S-wave velocity in geotechnical applications were wave stacking, P-correlated-S, and S-correlated-S methods [31]. The last one, S-correlated-S method, is also known as cross-correlation method; a window containing the S-wave arrival is cross-correlated against the next record to locate the best fit [31]. In P-correlated-S technique, P-wave arrival is determined first; then, the arrival of S-wave is identified by searching down the record to find a value that is approximately equal to or greater than the square of the energy of the P-waveform [31]. However, these methods were not successful to determine the S-wave velocity in the experimental phase of this work. The reason was the overlapping S-wave arrivals by P-wave arrivals. Analyses leading to this conclusion were intentionally excluded from the discussion so as not to blur the objective by affecting the focus of this study. In short, techniques which were successful in geotechnical applications did not produce repeatable results in concrete.

Using Hilbert transform algorithm provides another method to determine the P- and S-wave velocities by rectifying the ultrasonic pulse waveform [34]. Putting in simpler terms, all positive frequencies of a signal get a −90° phase shift whereas all negative frequencies get a +90° phase shift. So, Hilbert transform is just a filter that changes the phase of the spectral component depending on the sign of their frequency. It only affects the phase of the signal; it has no effect on the amplitude at all. By this method the rapid oscillations are removed,

* Tel.: +90 252 211 1920; fax: +90 252 223 9161.
E-mail address: rbirgul@gmail.com.

0008-8846/$ – see front matter © 2009 Elsevier Ltd. All rights reserved.
doi:10.1016/j.cemconres.2009.05.003

Table 1
Physical and chemical properties of Portland cement.

Chemical analysis (%)	
CaO	65.6
SiO_2	21.2
Al_2O_3	4.5
Fe_2O_3	2.6
MgO	1.9
SO_3	2.6
Equivalent Na_2O	0.48
Loss on ignition	1.5
Insoluble residue	0.37
Physical properties	
Specific gravity	3.06
Fineness (Blaine) (cm^2/g)	3720

producing an envelope of the waveform. This characteristic of the transformation gives the opportunity to observe the amplitude changes in the waveform such that the arrival of S-wave could be distinguished.

The objective of this work is to utilize Hilbert transform like a filter to process the signals acquired from the experiments and examine if the technique produces repeatable and reliable results. Since the technique yields only an envelope of the gathered data it seems to be a simple yet rewarding technique for analysing the signals.

2. Experimental program

2.1. Material properties

The Portland cement used in this study was labelled as ASTM C 150 Type I Portland cement. The physical and chemical properties of the Portland cement are listed in Table 1. The fine aggregate was river sand and the coarse aggregate was crushed stone. The physical properties of aggregates are provided in Table 2. The gradation of both aggregates was also determined by sieve analysis and presented in Fig. 1. As seen in Fig. 1 the nominal coarse aggregate size was 20 mm.

2.2. Mixture proportions

The concrete mixture proportions per cubic meter was 390 kg of cement, 690 kg of fine aggregate, 992 kg of coarse aggregate, and 175 kg of water with a w/c ratio of 0.45. Each cubic meter of the mix also included 248 mL of air entraining agent and 991 mL of retarding agent. The mix produced a slump of 10 mm with 5.7% of entrained air.

2.3. Test specimen and mixture properties

The specimen consisted of a portion of a bridge deck that was manufactured with a typical deck thickness value of 230 mm and with the diameters of 10 and 16 mm reinforcements to simulate the field conditions more realistically. Fig. 2 shows the cross sections of the test specimen in both directions. The length of 1500 mm and the width of 1000 mm were arbitrarily chosen to construct a deck specimen that could be handled in the laboratory. The placement of reinforcement also followed the field applications; primary reinforcements were placed with a 200 mm spacing between them; hence, there were 7 spaces in the long direction of the lab-deck as shown in Fig 2a. Likewise, secondary reinforcements were placed 290 mm apart from each other; therefore, 3 spaces between the reinforcements existed in the short direction as shown in Fig 2b.

Table 2
Physical properties of aggregates.

	Fine aggregate	Coarse aggregate
Unit weight (kg/m^3)	1.52	1.39
Specific gravity (SSD)	2.56	2.61
Absorption (%)	1831	1384

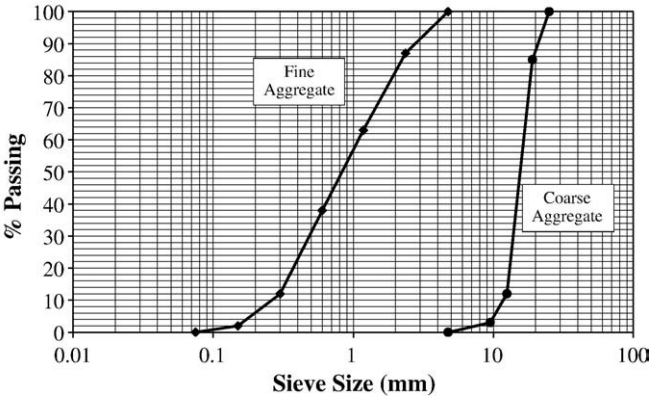

Fig. 1. Sieve analysis of aggregates.

In addition to this lab-deck specimen, 150×300 mm cylindrical specimens were also cast from the same batch to obtain mechanical properties. The compressive strength of the mixture was determined as 35.83, 40.34, and 41.02 MPa at 7, 14, and 28 days, respectively following the ASTM C 39 standard. In addition to the compressive strength, the modulus of elasticity and Poisson's ratio of the mixture were also determined following the ASTM C 469 standard and were found as 28.4 GPa and 0.24, respectively at the end of 28 days. Finally, the density of the concrete mixture was also determined as 2190 kg/m^3 at the end of 28 days.

2.4. Test equipment

The USWV measuring system consists of pulser/receiver unit (Panametrics 5058 PR), a personal computer with a 100 MHz 2-channel digital oscilloscope board (Gage CompuScope 2125) and a pair of normal incidence shear wave transducers.

In the pulser/receiver unit, the pulser settings prescribing the pulse voltage and damping, receiver settings prescribing the gain, attenuation, low- and high-pass filters were kept fixed throughout the measurements. The software of the oscilloscope board was configured to digitize the recorded wave signal at 0.02 ms time increments thus a

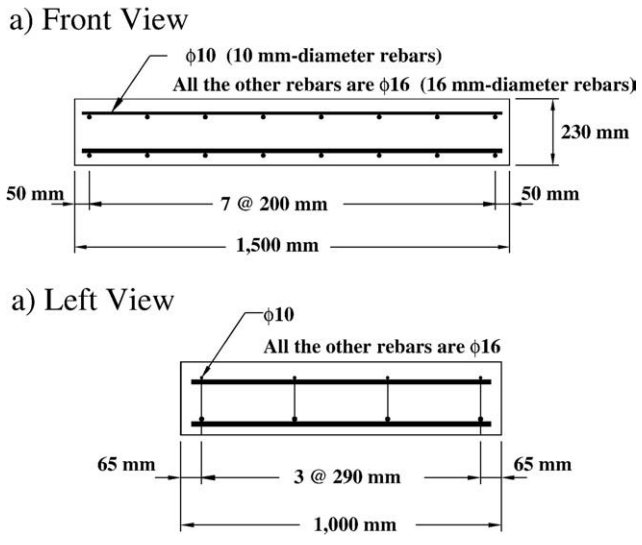

Fig. 2. Experimental test specimen.

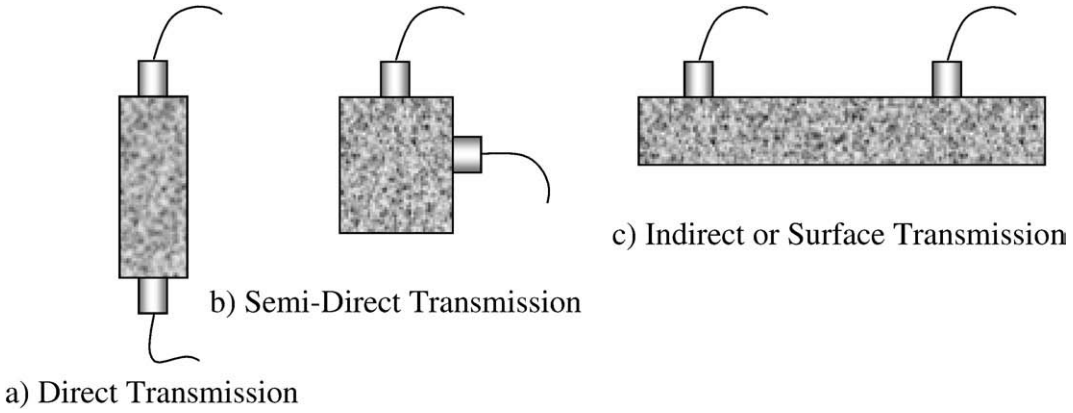

Fig. 3. Transmission types.

50 MHz sampling frequency. Moreover, the acquisition system was synchronized to the pulser so that the data collection started at the exact time the pulse was applied. Therefore, there would be no uncertainty in the time of pulse application. However, arrival times could differ due to the presence of noise superposed with the wave signal. The normal incidence shear wave transducers had a diameter of 25 mm and a centre frequency of 100 kHz. It was essential that there be adequate acoustical couplant between the lab-deck specimen and the face of each transducer. The surfaces are not sufficiently smooth for most of the concrete works. Since shear waves cannot propagate in a liquid medium a very viscous couplant is necessary. Therefore, honey was introduced as the coupling medium between the face of the transducer and the lab-deck specimen to ensure good acoustical contact.

2.5. Test procedure

In ultrasonic testing, transducers are utilized both to generate pulses and to detect the response of the specimen. The arrangement of transducers and the specimen determines the type of experiment. As shown in Fig. 3, there are mainly three types of arrangements [12]:

1) Direct transmission
2) Semi-direct transmission
3) Indirect or surface transmission

It is clear from Fig. 3 that the most desirable arrangement is the direct transmission type since maximum energy of the pulse is transmitted and received with this arrangement; the semi direct transmission type can also be used satisfactorily as long as the transducers are not placed too far apart and reinforcement concentrations are avoided. The indirect or surface transmission type is the least satisfactory method because the amplitude of the received signal may only be about 3% or less than that received by the direct transmission method [1,12,35]. However, the only practical option to obtain waveforms from an actual bridge deck is to use the indirect (surface) transmission arrangement. Therefore, wave velocity measurements were performed with an indirect transducer arrangement on the lab-deck surface to imitate the real life conditions.

Before the measurements, the surface of the lab-deck was ground to smooth it out but not eliminate the tining. The smooth surface is important to ensure adequate transducer contact. As explained in the Test Equipment section, there was a pair of shear wave transducers: a pulser and a receiver. Indirect wave velocity measurements were taken on the lab-deck by using a plexiglass template that had been designed for precise placement of the pulsing and receiving transducers. Without this template, one would have to mark the prepared surface by measuring the distances for the pulser and the receiver locations and then complete the wave measurements. This application would slow down the wave measurements and induce errors in the gathered data. To avoid such problems, a template, manufactured from plexiglass material, seemed to be a reasonable solution. A rectangular area with the dimensions of 200 mm by 500 mm was obtained from a plexiglass material; the length was

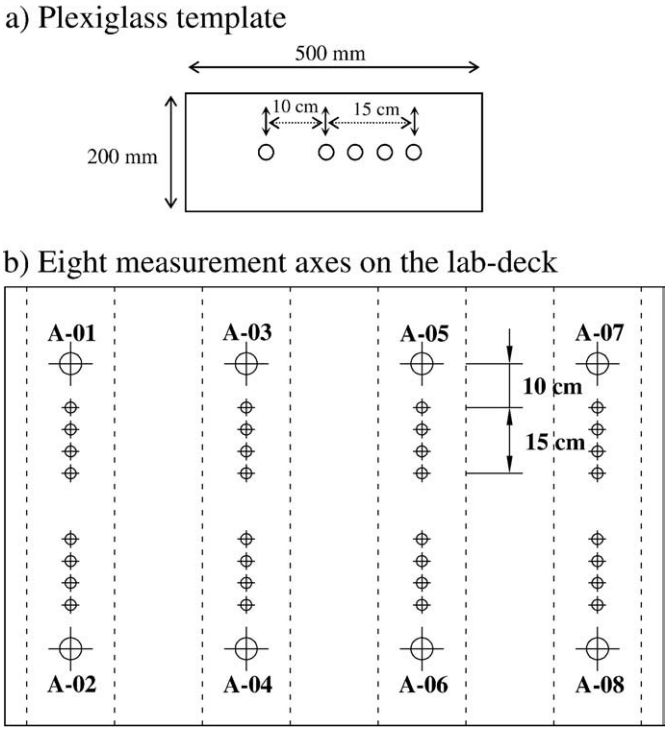

Fig. 4. Experimental setup on the deck (plan view) for wave velocity measurements.

Table 3
P-wave arrival time (μs).

Transducer spacing (cm)	Measurement axes							
	A-01	A-02	A-03	A-04	A-05	A-06	A-07	A-08
10	21.04	19.40	18.96	20.34	20.52	21.00	20.05	20.02
15	31.62	30.14	29.52	31.50	32.00	31.50	33.00	32.50
20	46.88	43.20	44.12	43.40	43.00	45.00	45.00	44.00
25	56.04	55.06	54.16	56.00	56.04	56.00	56.30	56.09

Table 4
S-wave arrival time (μs).

Transducer spacing (cm)	Measurement axes							
	A-01	A-02	A-03	A-04	A-05	A-06	A-07	A-08
10	42.32	36.80	43.38	42.56	44.42	45.12	42.70	41.14
15	63.52	61.40	64.66	62.02	63.46	63.22	69.06	65.32
20	83.60	81.90	84.50	81.04	84.14	87.06	88.52	87.58
25	108.40	100.64	103.12	102.80	104.08	102.52	106.94	105.30

deliberately chosen to be 500 mm to span the half-width of the experimental lab-deck. Fig. 4 a depicts where the holes were made on the template. The template corresponded to a measurement axis on the lab-deck; there were four measurement locations to obtain the waveforms from one axis. The labelling from A-01 through A-08 in Fig. 4b denotes the eight measurement axes and corresponds to the results given in Table 3 and Table 4. The dotted lines show the locations of reinforcements. Bigger circles were the pulsing transducer locations whereas smaller circles were the receiving transducer locations. Even though all of the holes had 25 mm diameter, pulser locations were drawn bigger than the receiver locations to distinguish their positions on the lab-deck. The holes for receivers were spaced at 5 cm distances to each other; the nearest receiver and pulser distance was 10 cm. When conducting the measurements, one would secure the template on the lab-deck surface by using duct tapes. Then, the pulser was placed in its location on the template. Next, the receiver was positioned in the first hole that was the nearest hole to the pulser location. At each receiver location, three measurements were gathered to eliminate user introduced errors. When the measurements were completed, the receiver was moved to the next hole and the waveform measurements were repeated. After completing a measurement axis that consists of four receiver locations, the template was moved to the next location and the above procedure was applied all over again.

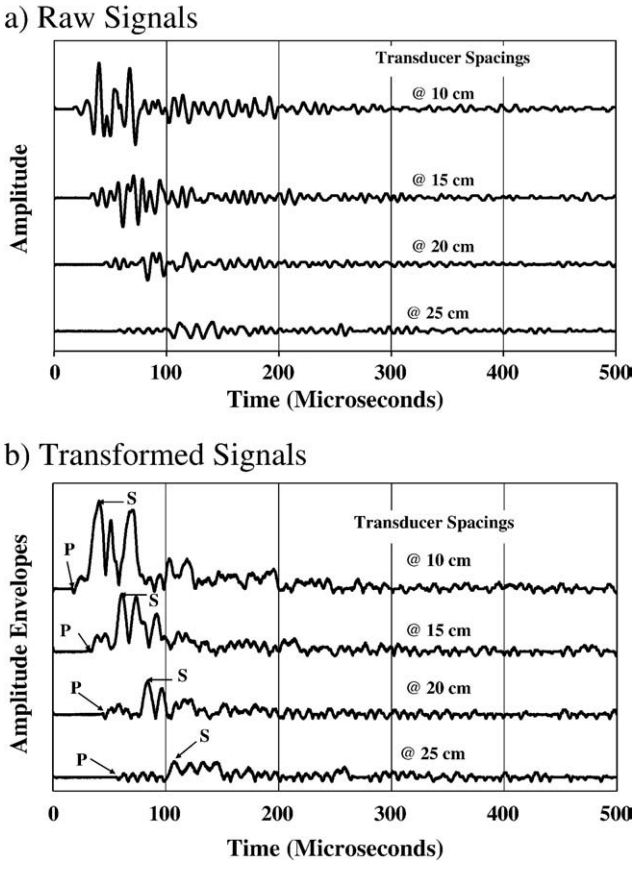

Fig. 5. P- and S-wave arrival times for Axis A-01.

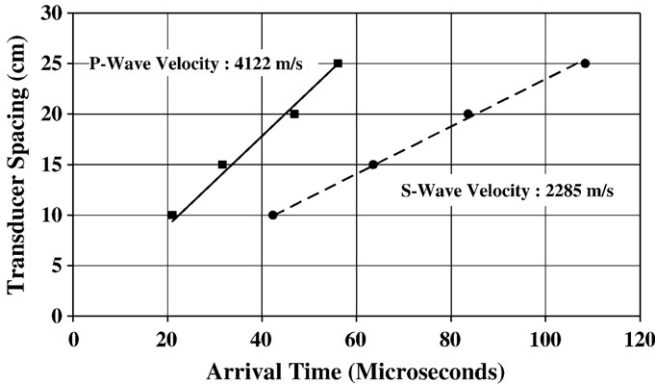

Fig. 6. P- and S-wave velocity calculation for Axis A-01.

3. Results

3.1. P- and S-wave arrival time detections by Hilbert transformation

The raw signals obtained from a typical data acquisition phase for the four measurement points located in Axis-01 (A-01) are presented in Fig. 5a. As seen in the figure, the amplitudes of the waveforms decayed as the distance between pulser and receiver increases.

Fig. 5b gives the Hilbert transformation of the raw signals. Basically, transformation envelops the signal. As presented in Fig. 5b, the first disturbances are located as P-wave arrivals whereas the second disturbances at the sharp amplitude increases are located as S-wave arrivals. The arrival times for P- and S-waves for all the measurement axes are presented in Table 3 and Table 4, respectively.

3.2. P- and S-wave velocity calculation

P- and S-wave velocity calculations were carried out for the measurements obtained from eight axes on the lab-deck. For each axis, transducer spacing versus arrival times were plotted as shown in Fig. 6 for the axis A-01 and the calculated slopes yielded the P- and S-wave velocities for those particular measurements. Table 5 presents the P- and S-wave velocities for each axis scanned. The mean P-wave velocity for the lab-deck was calculated as 4181 m/s with a coefficient of variation of 0.9%. The mean S-wave velocity was found to be 2417 m/s with a coefficient of variation of 4.3%.

3.3. Calculation of modulus of elasticity and Poisson's ratio

At the macro level, assuming the concrete as a homogeneous and isotropic material, in fact it is not at the micro or meso level [36], the

Table 5
P- and S-wave velocities (m/s).

Velocity	Measurement axes							
	A-01	A-02	A-03	A-04	A-05	A-06	A-07	A-08
P-wave	4122	4160	4225	4203	4217	4210	4137	4176
S-wave	2285	2349	2510	2501	2504	2535	2338	2318

two elastic constants, modulus of elasticity and Poisson's ratio, can be calculated by the following:

$$v = \frac{1 - 2(V_S/V_P)^2}{2 - 2(V_S/V_P)^2} \quad (1)$$

$$E = 2\rho V_s^2(1 + v) \quad (2)$$

With the P- and S-wave velocities that are experimentally measured, the two constants are calculated by the equations given above as 31.9 GPa for modulus of elasticity (E) and 0.25 for Poisson's ratio (v). These values were 28.4 GPa for E and 0.24 for v as determined through static testing on the 150×300 mm cylindrical specimens. The Poisson's ratio values could be practically called equal for both cases, static and dynamic measurements; on the other hand, the modulus of elasticity value from the wave velocity measurements of the deck is about 12% greater than that of the measured on the concrete cylinders. This result agrees quite well with the literature; it is already known that the value of dynamic elasticity modulus measured by resonant frequency methods such as ASTM C 215-02 is about 10% higher than the value obtained from conventional stress–strain tests [1]. Malhotra and Carino [1] reported a detailed comparison of dynamic and static moduli of elasticity based on the previous works of other researchers.

4. Conclusions

In this study ultrasonic pulse measurements on a laboratory produced bridge deck specimen were performed and applicability of Hilbert transformation when trying to determine the P- and S-wave velocities was investigated. The obtained results showed that analysis of the waveform via Hilbert Transformation produced reliable and repeatable results. In addition, experimentally obtained P- and S-wave velocities could be used to assess the elastic properties of concrete material. This aspect might come in handy when testing in-situ concrete for quality control and quality assurance of the material.

Acknowledgements

The author wishes to express his deep appreciation to the Civil and Environmental Engineering Department of Wayne State University of Detroit, MI for the financial support to complete this study. The author is also grateful to Prof. Haluk Aktan and Assoc. Prof. Ozgur Yaman for their constructive criticisms. Invaluable help from Mr. Jason Rutyna and Mr. Hakan Karaca are greatly appreciated in obtaining the experimental data.

References

[1] V.M. Malhotra, N.J. Carino, Handbook on non-destructive testing of concrete, CRC Press, Boca Raton, FL, 1991.
[2] J. Krautkramer, H. Krautkramer, Ultrasonic testing of materials, Springer-Verlag, Berlin, 1990.
[3] M. Sansalone, W.B. Streett, Impact-Echo Non-Destructive Evaluation of Concrete and Masonry, Bullbrier Press, Ithaca, NY, 1997.
[4] J.F. Doyle, Wave Propagation in Structures, Springer-Verlag, New York, 1989.
[5] ACI 228.2R-98, Non-destructive Test Methods of Evaluation of Concrete in Structures, ACI Committee 228.
[6] T. Öztürk, J.R. Rapoport, J.S. Popovics, S.P. Shah, Monitoring the setting and hardening of cement-based materials with ultrasound, Concr. Sci. Eng. 1 (2) (1999) 83–91.
[7] W.G. Wong, P. Fang, J.K. Pan, Dynamic properties impact toughness and abrasiveness of polymer-modified pastes by using nondestructive tests, Cem. Concr. Res. 33 (9) (2003) 1371–1374.
[8] R. Birgul, F.M.W. Al-Shammari, I.O. Yaman, M.H. Aktan, Acoustic emission evaluation of concrete culverts, Res. Nondes Eval. 15 (4) (2004) 191–208.
[9] S. Nazarian, M. Baker, K. Crain, Assessing quality of concrete with wave propagation techniques, ACI Mater. J. 91 (4) (1997) 296–305.
[10] I.O. Yaman, R. Birgul, H.M. Aktan, N. Hearn, J.F. Staton, Test method for appraising future durability of new concrete bridge decks, Transport. Res. Rec. 1798 (2002) 56–63.
[11] I.O. Yaman, H.M. Aktan, J.F. Staton, Relationship between concrete permeability and ultrasonic pulse velocity, TRB 80th Annual Meetings, January 2001.
[12] I.O. Yaman, G. Inci, N. Yesiller, H.M. Aktan, Ultrasonic pulse velocity in concrete using direct and indirect transmission, ACI Mater. J. 98 (6) (2001) 450–457.
[13] A. Maji, S.P. Shah, Process zone and acoustic-emission measurements in concrete, Exp. Mech. 28 (1988) 27–33.
[14] E.N. Landis, S.P. Shah, Frequency-dependent stress wave attenuation in cement-based materials, J. Eng. Mech-ASCE 121 (6) (1995) 737–742.
[15] M.T. Liang, J. Wu, Theoretical elucidation on the empirical formulae for the ultrasonic testing method for concrete structures, Cem. Concr. Res. 32 (11) (2002) 1763–1769.
[16] Y. Berthaud, Damage measurements in concrete via an ultrasonic technique part II modeling, Cem. Concr. Res. 21 (2–3) (1991) 219–228.
[17] I.O. Yaman, N. Hearn, H.M. Aktan, Active and nonactive porosity in concrete-part I: experimental evidence, Mater. Struct. 35 (2002) 102–109.
[18] J.R. Rapoport, J.S. Popovics, K.V. Subramaniam, S.P. Shah, The use of ultrasound to monitor the stiffening process of Portland cement concrete with admixtures, ACI Mater. J. 97 (6) (2000) 675–683.
[19] A. Gibson, J.S. Popovics, Lamb wave basis for impact-echo method analysis, J. Eng. Mech. ASCE 131 (2005) 438–443.
[20] J.S. Popovics, W. Song, J.D. Achenbach, J.H. Lee, R.F. Andre, One-sided stress wave velocity measurement in concrete, J. Eng. Mech. ASCE 124 (1998) 1346–1353.
[21] K. Warnemuende, H.C. Wu, Actively modulated acoustic nondestructive evaluation of concrete, Cem. Concr. Res. 34 (4) (2006) 563–570.
[22] E.G. Brignoli, M. Gotti, K.H. Stokoe II, Measurement of shear waves in laboratory specimens by means of piezoelectric transducers, Geotech. Test J. ASTM 19 (4) (1996) 384–397.
[23] N. Krstulovic-Opara, R.D. Woods, N. Al-Shayea, Nondestructive testing of concrete structures using the Rayleigh wave dispersion method, ACI Mater. J. 93 (1) (1996) 75–86.
[24] K.O. Addo, P.K. Robertson, Shear wave velocity measurement of soils using Rayleigh waves, Can. Geotech. J. 29 (1992) 558–568.
[25] J.F. Evans, Seismic model experiments with shear waves, Geophysics 24 (1959) 41–48.
[26] A.G. Winbow, Compressional and shear arrivals in a multipole sonic log, Geophysics 50 (7) (1985) 1119–1126.
[27] M.L. Greenberg, J.P. Castagna, Shear wave velocity estimation in porous rocks: theoretical formulation, preliminary verification and applications, Geophys. Prospect. 40 (1992) 195–209.
[28] S. Crampin, A review of wave motion in anisotropic and cracked elastic media, Wave Motion 3 (1981) 343–391.
[29] C.P. Abbiss, Shear wave measurements of the elasticity of the ground, Geotechnique 31 (1) (1981) 91–104.
[30] J.E. White, Seismic Waves, Radiation, Transmission and Attenuation, 1st ed. McGraw-Hill Book Company, New York, 1965.
[31] M.E. Willis, M.N. Toksöz, Automatic P and S velocity determination from full waveform digital acoustic logs, Geophysics 48 (12) (1983) 1631–1644.
[32] R. Chammas, O. Abraham, Ph. Côte, H.A. Pedersen, J.-F. Semblat, Characterization of heterogeneous soils using surface waves: homogenisation and numerical modelling, ASCE Int. J. Geomech. 3 (1) (2003) 55–63.
[33] D. Jongmans, D. Demanet, The importance of surface waves in vibration study and the use of Rayleigh waves for estimating the dynamic characteristics of soils, Eng. Geol. 34 (1993) 105–113.
[34] G.G. Leisk, A. Saigal, Digital computer algorithms to calculate ultrasonic wave speed, Mater. Eval. 54 (7) (1996) 840–843.
[35] I.O. Yaman, G. Inci, N. Yesiller, H.M. Aktan, Ultrasonic pulse velocity in concrete using direct and indirect transmission, ACI Mater. J. 98 (6) (2001) 450–457.
[36] I.O. Yaman, H.M. Aktan, N. Hearn, Active and nonactive porosity in concrete-part II: evaluation of existing models, Mater. Struct. 35 (2002) 110–116.